Theoretical calculations of the total and ionization cross sections for electron impact on some simple biomolecules

Minaxi Vinodkumar,[1,*] K. N. Joshipura,[2] Chetan Limbachiya,[3] and Nigel Mason[4]
[1]*V. P. & R. P. T. P. Science College, Vallabh Vidyanagar-388120, India*
[2]*Department of Physics, Sardar Patel University, Vallabh Vidyanagar-388120, India*
[3]*P. S. Science College, Kadi—382 715, India*
[4]*Department of Physics & Astronomy, Open University, Milton Keynes, MK7 6AA, United Kingdom*
(Received 2 June 2006; published 28 August 2006)

In this paper we report total cross sections (TCS), Q_T, total elastic cross sections, Q_{el}, and total ionization cross section, Q_{ion} for electron impact on water, formaldehyde, formic acid, and the formyl radical from circa 15 eV to 2 KeV. The results are compared where possible, with previous theoretical and experimental results and, in general, are found to be in good agreement. The total and elastic cross sections for HCHO, HCOOH, and CHO radical are reported.

DOI: 10.1103/PhysRevA.74.022721 PACS number(s): 34.80.Bm

I. INTRODUCTION

It is well established that the most important damage induced in DNA by ionizing radiation is that arising from double strand breaks (DSB) and clustered lesions, since these have the greatest potential for producing long lasting biological effects. Clustered lesions and strand breaks occur most readily where primary radiation tracks interact directly with the DNA causing local base damage, a picture recently supported by both direct experimental evidence and modeling studies [1]. The genotoxic effects of ionizing radiation in living cells are not only produced by the direct impact of the primary high energy projectiles but may also be induced by the secondary species generated by primary ionizing radiation as it passes through the cell. Indeed recent studies suggest that DNA may be directly damaged by secondary electrons [2]. This hypothesis, although still the subject of considerable debate, has been supported by several recent experiments showing how low energy electrons incident on the molecular components of DNA may lead to efficient molecular dissociation [3]. However electron scattering experiments with biomolecules (e.g., nucleotide bases, nucleosides, amino acids, peptides) in the gas phase remain sparse since there are many practical difficulties in preparing well-characterized pure gas targets of these molecules and it is difficult to determine target number densities. Hence there is need for more comprehensive theoretical investigations of electron scattering from such targets, with the models of radiation damage requiring an evaluation/estimation of the various cross sections for such biomolecules.

H_2O is perhaps the most important molecule in biological systems. The water content of the human body is about 60% by weight [4]. Any radiation that penetrates the human body produces secondary electrons, with appreciable kinetic energy, that will subsequently interact with water to liberate free radicals (e.g., OH) which lead to various biological effects in the human body. Electron interactions with water have therefore been studied extensively [5–7] although there remain several questions as to the magnitude of many cross sections. Hence in the present project we have started our investigations by determining electron scattering cross sections in water viz. total (complete), elastic and ionization from threshold to 2 KeV. Such data may be tested with previous evaluations and therefore act as something of a calibrant for the other molecules.

Formaldehyde has been proposed as a key molecule in prebiotic evolution because of the ease with which it may be formed under simulated prebiotic conditions and its ability to condense with itself to form carbohydrates [8]. Its astrobiological potential has recently been underlined in spectacular fashion by discovery of formaldehyde in the interstellar clouds in our galaxy [9,10]. To date electron impact studies have been limited to *ab initio* elastic scattering calculations using the *R* matrix at low energies by Savinder and Baluja [11], while ionization cross sections have been reported by Kim *et al.* [12]. However no experimental or theoretical data for Q_T and Q_{el} have been reported in the present energy range.

Formic acid (HCOOH), the simplest organic acid, has also been recently identified in the interstellar medium (ISM) and in the coma of the Hale-Bopp comet [13,14]. It is therefore speculated that formic acid be a key compound in the formation of biomolecules such as acetic acid (CH_3COOH) and glycine (NH_2CH_2COOH) in the ISM [15]. Moreover formic acid and glycine are the simplest building blocks of those biomolecules which serve as model systems for studying the properties of larger and more complex amino acids especially with respect to their behavior during exposure to high energy radiation. Amino acids are the building blocks of proteins and DNA, hence it is necessary to understand the formation mechanisms of amino acids in space where more complex, biologically important molecules might be located and where the conditions for the development of life exists [15]. Despite the importance of electron scattering from formic acid, we are not aware of any theoretical calculations or experimental data.

Formyl radical is formed during the oxidation of hydrogen-containing organic compounds [16] and has been detected in interstellar molecular clouds [17]. As with formic

*Email address: minaxivinod@yahoo.co.in

TABLE I. Ionization potential (I) for targets studied.

Target	I(eV)
H_2O	12.62
HCHO	10.88
HCOOH	11.33
CHO	09.20

acid we are not aware of any experimental data for Q_T and Q_{el} for this radical. However Kim and co-workers have reported calculated ionization cross sections [12].

In this paper we report results on the total, total elastic, and ionization cross sections for water, formaldehyde, formic acid, and the formyl radical (CHO) from close to the ionization threshold to 2 keV. The total cross sections provide a useful sum-check of elastic and inelastic scattering cross sections. The ionization potentials of these targets are shown in Table I.

II. THEORETICAL METHODOLOGY

We will only briefly describe the theoretical formalism employed to determine the Q_T, Q_{el}, and Q_{ion} for the impact of electrons on the molecules and radical studied, a more detailed description can be found in our earlier papers [18–23] and references therein. Our aim in this paper is to calculate various TCSs and to investigate their contributions relative to the total (complete) cross sections for the chosen targets. We have employed the well-known spherical complex optical potential formalism (SCOP). The complex potential calculation for electron scattering can provide total elastic cross sections Q_{el} and its inelastic counterpart, Q_{inel} such that

$$Q_T(E_i) = Q_{el}(E_i) + Q_{inel}(E_i). \tag{1}$$

For a polar molecule such as H_2O, we have also determined the dipole rotational excitation cross section $Q_{01}(D,E_i)$ [24]. We can then define the grand total cross section by

$$Q_{TOT}(E_i) = Q_T(E_i) + Q_{01}(D,E_i). \tag{2}$$

The dipole rotational excitation $Q_{01}(D,E_i)$ is calculated using the first Born approximation for a molecular dipole of strength D.

Our calculation for the TCSs [Eq. (1)] is based on a complex scattering potential, generated from spherically averaged charge densities of the target. We have used single center approach for H_2O molecule. The charge density of O and H atoms are expanded at the center of mass of the molecule. In contrast formaldehyde, HCHO, and formic acid (HCOOH) are multicenter systems. We have used the multicenter group additivity rule [18]. Here, the charge density of lighter hydrogen atom is expanded at the center of heavier atom (carbon or oxygen). The single-center molecular charge density is then obtained by a linear combination of constituent atomic charge densities, renormalized to account for covalent molecular bonding. The justification for group additivity comes from relatively larger C-O bond length compared to C-H or O-H bond lengths in these molecules [25]. The molecular charge density thus obtained is employed to construct a complex optical potential V_{opt}, given by

$$V_{opt}(E_i,r) = V_R(E_i,r) + iV_I(E_i,r). \tag{3}$$

The real part V_R comprises of static potential (V_{st}), exchange potential (V_{ex}), and polarization potential (V_p) terms, as follows:

$$V_R(E_i,r) = V_{st}(r) + V_{ex}(E_i,r) + V_P(E_i,r). \tag{4}$$

We have used the analytical form of the static potential derived using the Hartree-Fock wave functions. For the exchange potential, we have used Hara's "free electron gas exchange model" [26]. For the polarization potential V_p, we have used parameter free model of correlation polarization potential which contains some multipole nonadiabatic corrections in the intermediate region and it smoothly approaches the correct asymptotic form for large r given by Zhang *et al.* [27]. The imaginary part V_I, also called the absorption potential V_{abs}, accounts for the total loss of scattered flux into all the allowed channels of electronic excitation and ionization. For V_{abs} we have used the model potential given by Staszewska [28], which is a quasifree, Pauli blocking, dynamic absorption potential. After generating the full complex potential given in Eq. (3) for a given electron-target system, we solve the Schrödinger equation to get complex phase shifts which are used to find the cross sections given in Eq. (1).

The total inelastic cross section, Q_{inel} cannot be measured directly. Q_{inel} can therefore be partitioned into two main contributions viz.

$$Q_{inel}(E_i) = \sum Q_{exc}(E_i) + Q_{ion}(E_i), \tag{5}$$

where the first term is the sum over total excitation cross sections for all accessible electronic transitions. The second term is the total cross section of all allowed ionization processes induced by the incident electrons. The first term arises mainly from the low-lying dipole allowed transitions for which the cross section decreases rapidly at higher energies. The first term in Eq. (5) therefore becomes progressively smaller than the second at energies well above the ionization threshold. By definition

$$Q_{inel}(E_i) \geqslant Q_{ion}(E_i). \tag{6}$$

Q_{ion} cannot be directly derived from Q_{inel} but may be estimated by the cross-section energy dependent ratio

$$R(E_i) = \frac{Q_{ion}(E_i)}{Q_{inel}(E_i)} \tag{7}$$

such that

$$0 < R \leqslant 1.$$

We require that $R=0$ when $E_i < I$. For a number of stable molecules such as O_2, H_2O, CH_4, SiH_4, etc., for which the experimental cross sections Q_{ion} are known accurately [29,30], the ratio R rises steadily as the energy increases above the threshold, and approaches unity at high energies. Thus,

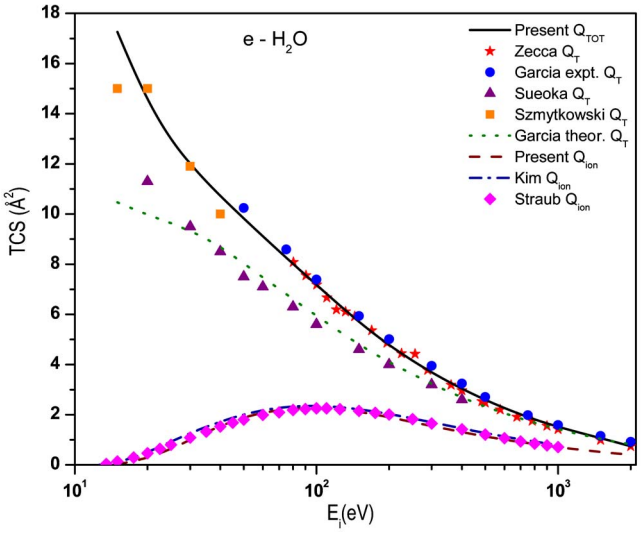

FIG. 1. (Color online) TCSs for $e-H_2O$ scattering. Solid line, present Q_{TOT}, Star, Zecca Q_T [4], Filled circle, Garcia expt. Q_T [32], Up triangle, Sueoka Q_T [6], Square, Szmytkowski Q_T [31], Dotted line, Garcia theo. Q_T [32]. Dashed line, present Q_{ion}, Dashdot line, Kim Q_{ion} [12], Diamond, Straub Q_{ion} [33].

$$R(E_i) = 0 \quad \text{for} \quad E_i \leq I$$
$$= R_P \quad \text{at} \quad E_i = E_P$$
$$= 1 \quad \text{for} \quad E_i > E_P, \tag{8}$$

where E_p stands for the incident energy at which the calculated Q_{inel} attains its maximum. R_p is the value of R at $E_i = E_p$, and we choose $R_p = 0.7$ to 0.8. This choice follows from the general observation that at energies close to peak of ionization, the contribution of the molecular Q_{ion} is about 70–80 % in the total inelastic cross sections Q_{inel}. This behavior is attributed to the faster fall of the first term ΣQ_{exc} in Eq. (5). For calculating the Q_{ion} from Q_{inel} we need R as a continuous function of energy for $E_i > I$; hence we represent the ratio R in the following manner:

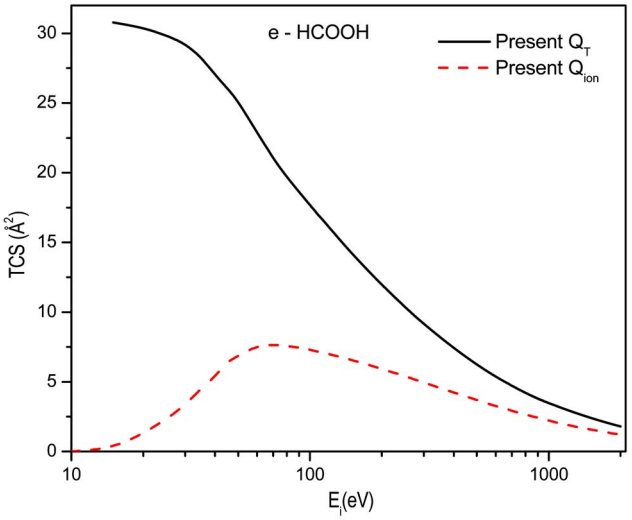

FIG. 3. (Color online) TCSs for $e-HCOOH$ scattering. Solid line, present Q_T. Dashed line, present Q_{ion}.

$$R(E_i) = 1 - f(U). \tag{9}$$

Presently the above ratio has been determined using the following analytical form [18,19]:

$$R(E_i) = 1 - C_1\left(\frac{C_2}{U+a} + \frac{\ln(U)}{U}\right), \tag{10}$$

where U is the dimensionless variable defined by

$$U = \frac{E_i}{I}. \tag{11}$$

The reason for adopting a particular functional form of $f(U)$ in Eq. (11) is the following. As E_i increases above I, the ratio

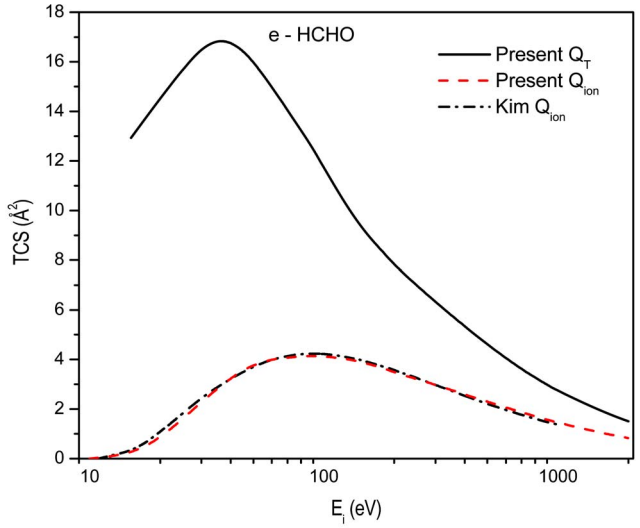

FIG. 2. (Color online) TCSs for $e-HCHO$ scattering. Solid line, present Q_T. Dashed line, present Q_{ion}, Dashdot line, Kim Q_{ion} [12].

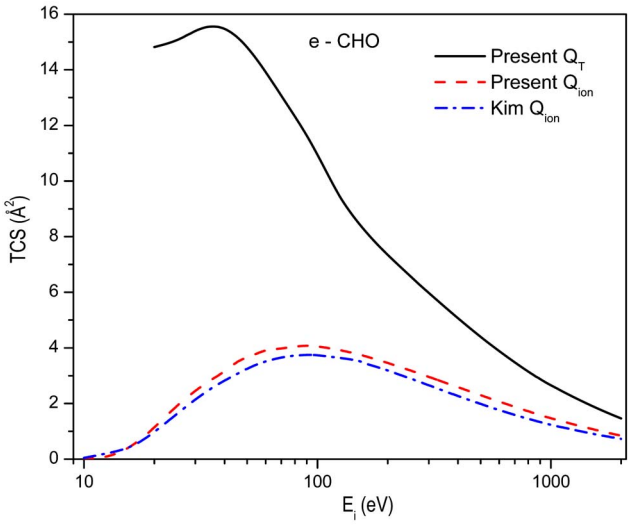

FIG. 4. (Color online) TCSs for $e-CHO$ scattering. Solid line, present Q_T. Dashed line, present Q_{ion}, Dashdot line, Kim Q_{ion} [12].

TABLE II. Total elastic, ionization and grand total cross sections (10^{-16} cm^2) for e-H_2O.

Energy (eV)	Q_{el}	Q_{ion}	Q_{TOT}
15	5.64	0.02	17.25
20	5.04	0.25	14.46
25	4.67	0.63	12.96
30	4.39	0.99	11.99
35	4.16	1.30	11.28
40	3.95	1.55	10.72
45	3.76	1.74	10.24
50	3.59	1.88	9.82
55	3.43	1.99	9.45
60	3.30	2.08	9.11
70	3.07	2.18	8.52
80	2.87	2.24	8.02
90	2.69	2.26	7.57
100	2.53	2.21	7.17
125	2.20	2.11	6.35
150	1.95	2.01	5.70
175	1.77	1.90	5.18
200	1.64	1.70	4.77
250	1.45	1.55	4.14
300	1.31	1.31	3.68
400	1.11	1.14	3.03
500	0.96	1.01	2.59
600	0.85	0.91	2.26
700	0.76	0.83	2.01
800	0.68	0.76	1.81
900	0.61	0.71	1.65
1000	0.57	0.51	1.52
2000	0.35	0.40	0.74

TABLE III. Total elastic, ionization and complete cross sections (10^{-16} cm^2) for e-HCHO.

Energy (eV)	Q_{el}	Q_{ion}	Q_T
15	11.9	0.16	12.9
20	12.8	0.83	14.5
25	12.9	1.60	15.7
30	12.8	2.28	16.6
35	12.4	2.82	16.9
40	11.8	3.24	16.8
45	11.0	3.55	16.4
50	10.4	3.78	16.0
60	9.15	4.01	15.0
70	8.23	4.07	14.1
80	7.54	4.12	13.2
90	6.96	4.14	12.5
100	6.29	4.13	11.7
125	4.77	4.03	10.2
150	4.13	3.85	9.12
175	3.76	3.69	8.43
200	3.52	3.48	7.81
250	3.14	3.21	6.97
300	2.85	2.97	6.31
400	2.40	2.59	5.32
500	2.07	2.30	4.60
600	1.82	2.06	4.05
700	1.62	1.86	3.61
800	1.46	1.70	3.26
900	1.32	1.57	2.97
1000	1.21	1.45	2.73
2000	0.66	0.83	1.50

R increases and approaches 1, since the ionization contribution rises and the discrete excitation term in Eq. (5) decreases. The discrete excitation cross sections, dominated by dipole transitions, fall off as $\ln(U)/U$ at high energies. Accordingly the decrease of the function $f(U)$ must also be proportional to $\ln(U)/U$ in the high range of energy. However, the two term representation of $f(U)$ given in Eq. (10) is more appropriate since the first term in the square brackets ensures a better energy dependence at low and intermediate E_i. Eq. (10) involves dimensionless parameters C_1, C_2, and a, that reflect the target properties. The three conditions stated in Eq. (8) are used to determine these three parameters. To implement the third condition, we first assume $a=0$ and consider a two-parameter expression in Eq. (10). We therefore employ the first two conditions of Eq. (8) to evaluate the C parameters. The two parameter expression is then used to obtain the value of R at a high energy $E_i=10E_p$, and are employed in the third condition of Eq. (8).

This method discussed through Eqs. (6)–(10) is called our complex scattering potential—ionization contribution, CSP—ic.

III. RESULTS AND DISCUSSIONS

The presently calculated Q_{TOT} and Q_{ion} for H_2O and Q_T and Q_{ion} for HCHO, HCOOH, and the CHO radical are shown in Figs. 1–4, where comparisons are made with earlier data where available. Numerical values of Q_{el}, Q_{ion}, and Q_{TOT} for H_2O are presented in Table II and Q_{el}, Q_{ion}, and Q_T for the rest of the targets in Tables III–V. However, we have not plotted the total elastic cross sections for any of the targets investigated here, since no theoretical or experimental data is available for comparison. We will now discuss each data set in turn.

Figure 1 compares our calculated values of Q_{TOT} and Q_{ion} for electron scattering from water with available data. Our Q_{TOT} values agree very well with the experimental results of Zecca, Szmytkowski, and Garcia [5,31,32], while the experimental values of Sueoka [6] and the theoretical values of Garcia [32] are lower compared to other data. Our Q_{ion} values are in excellent agreement with theoretical values of Kim [12] and the experimental results of Straub *et al.* [33]. Apart from the results shown here, there are vast amount of cross section data that exists in literature for this molecule [34–39], which are not included in this figure to maintain the

TABLE IV. Total elastic, ionization, and complete cross sections (10^{-16} cm^2) for *e*-HCOOH.

Energy (eV)	Q_{el}	Q_{ion}	Q_T
15	30.3	0.40	30.77
20	28.6	1.33	30.39
25	26.3	2.36	29.85
30	24.2	3.40	29.27
35	21.7	4.49	28.26
40	18.6	5.41	27.03
45	16.3	6.36	26.06
50	14.7	6.86	25.11
60	11.8	7.48	22.88
70	9.34	7.63	21.02
80	8.85	7.58	19.69
90	8.12	7.45	18.62
100	7.54	7.29	17.68
125	6.41	6.91	15.73
150	5.58	6.55	14.19
175	4.98	6.22	12.97
200	4.50	5.92	11.96
250	3.79	5.39	10.36
300	3.26	4.95	9.14
400	2.56	4.23	7.40
500	2.10	3.69	6.22
600	1.77	3.26	5.36
700	1.53	2.93	4.71
800	1.35	2.65	4.21
900	1.21	2.42	3.79
1000	1.09	2.23	3.46
2000	0.56	1.21	1.80

TABLE V. Total elastic, ionization, and complete cross sections (10^{-16} cm^2) for *e*-CHO radical.

Energy (eV)	Q_{el}	Q_{ion}	Q_T
20	13.5	0.83	14.8
25	13.0	1.93	15.0
30	12.8	2.46	15.4
35	12.4	2.85	15.6
40	11.8	3.14	15.5
45	11.0	3.50	15.2
50	10.4	3.67	14.8
60	9.15	3.93	13.9
70	8.23	3.97	13.0
80	7.54	4.05	12.3
90	6.96	4.09	11.6
100	6.29	4.05	10.9
125	4.77	3.92	9.35
150	4.13	3.77	8.47
175	3.76	3.61	7.83
200	3.52	3.45	7.34
250	3.14	3.18	6.57
300	2.85	2.95	5.96
400	2.40	2.58	5.05
500	2.02	2.30	4.39
600	1.80	2.01	3.88
700	1.55	1.88	3.47
800	1.30	1.72	3.14
900	1.22	1.58	2.87
1000	1.99	1.47	2.46
2000	0.53	0.84	1.47

clarity. The present results for H_2O provide validation of the theoretical techniques adopted in this paper and provide us with some confidence in the validity of the cross sections derived for the other biomolecules for which we have no data with which to compare.

In Figures 2–4 we have plotted Q_T and Q_{ion} for HCHO, HCOOH, and CHO radical, respectively. There are no experimental or theoretical comparisons for formic acid. In case of HCHO our Q_{ion} values are in excellent agreement with the values of Kim while in the case of CHO radical our values are slightly higher than the values of Kim [12] throughout the range.

In Fig. 5 we compare the TCSs for all the targets investigated in the present study. The present study involves, as basic inputs, the molecular charge density and geometry of the target. The size of the molecule is determined by the total number of electrons and their arrangement. Figure 5 shows that Q_T increases with the increase in geometrical size of the molecule. However at very high energies the Q_T for all the targets tend to merge irrespective to the geometric size of the molecule. This is because at high energies, the interaction time of projectile with the target is significantly reduced, lowering the corresponding cross sections.

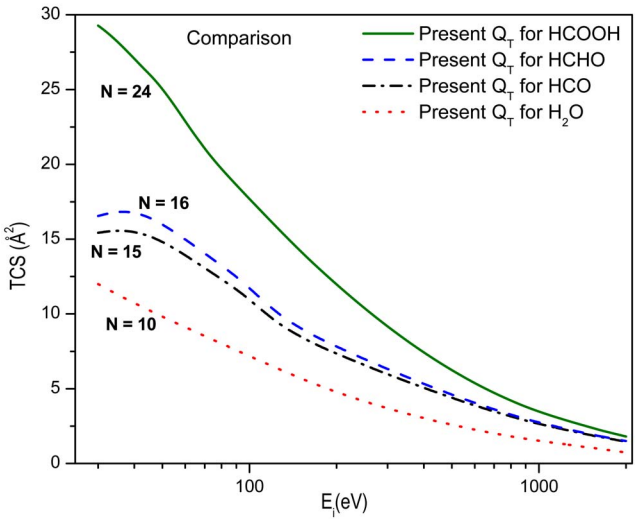

FIG. 5. (Color online) Comparison of the TCSs for different targets (*N*, number of target electrons). Solid line, present Q_T for HCOOH. Dashed line, present Q_T for HCHO. Dashdot line, present Q_T for HCO. Dotted line, present Q_T for H_2O.

IV. CONCLUSION

Low and intermediate energy behavior of cross sections is of much scientific interest because various elastic and inelastic phenomena occur in this range. The present SCOP theory, together with our CSP—ic method extends the scope of the traditional complex potential calculations and provides an estimate of important TCSs. This theory has been successfully employed to varieties of atomic and molecular targets [18–24]. The derived theoretical cross section Q_{inel} serve as the upper limit of the total ionization cross section.

In the present paper our emphasis has been to study electron scattering from the simplest molecules of biological interest, e.g., H_2O, HCHO, HCOOH, and the CHO radical. These molecules form the basis for other larger biomolecules which serve as model systems for studying the properties of amino acids, peptides, etc. Such studies play a vital role in understanding effects of radiation on complex biological systems.

The method adopted presently will now be employed to other larger biomolecules such as nucleotide bases and amino acids for which experiments are unlikely to be possible for some years.

ACKNOWLEDGMENTS

We thank the Royal Society of the UK for a their support for one of us (M.V.). K.N.J. is thankful for a research project funded by the Indian Space Research Organization, Bangalore.

[1] D. T. Goodhead, Int. J. Radiat. Biol. **65**, 117 (1994).
[2] B. Boudaiffa, P. Cloutier, D. Hunting, M. A. Huels, and L. Sanche, Science **287**, 1658 (2000).
[3] S. Ptasińska, S. Denifl, V. Grill, T. D. Märk, E. Illenberger, and P. Scheier, Phys. Rev. Lett. **95**, 093201 (2005).
[4] J. E. Turner, H. G. Partzke, R. N. Hamm, H. A. Wight, and R. H. Ritchie, Radiat. Res. **92**, 47 (1982).
[5] A. Zecca, G. P. Karwasz, S. Oss, R. Grisenti, and R. S. Brusa, J. Phys. B **20**, L133 (1987).
[6] O. Sueoka, S. Mori, and Y. Katayama, J. Phys. B **20**, 3237 (1987).
[7] O. Sueoka, S. Mori, and Y. Katayama, J. Phys. B **19**, L373 (1986).
[8] J. K. Quayle and T. Ferenci, Microbiol. Rev. **42**(2), 251 (1978).
[9] S. W. Fox and K Dose, *Molecular Evolution and the Origin of Life* (1972).
[10] S. L. Miller and L. E. Orgel, *The Origins of Life on the Earth* (*Prentice Hall*, Englewood Cliffs, New Jersey, 1974).
[11] Savinder Kaur and K. L. Baluja, J. Phys. B **38**, 3917 (2005).
[12] Y.-K. Kim, from NIST Web-Site, http:physics.nist.gov/PhysRefData/Ionization/EII table.html
[13] J. Ellder, P. Friberg, A. Hjalmarson, B. Hocglund, W. M. Irvine, L. E. B. Johansson, G. Rydbeck, and O. E. H. Rydbeck, Astrophys. J., Lett. Ed. **242**, L93 (1980).
[14] S. D. Rodgers and S. Charnley, Mon. Not. R. Astron. Soc. **320**, L61 (2001).
[15] T. Sedlacko, R. Balog, A. Lafosse, M. Stano, S. Matejeik, R. Azria, and E. Illenberger, Phys. Chem. Chem. Phys. **7**, 1277 (2006).
[16] R. S. Timonen, E. Ratajczak, and D. Gutman, J. Phys. Chem. **92**, 651 (1988).
[17] L. E. Snyder, J. M. Hollis, and B. L. Ulich, Astrophys. J. **208**, L91 (1976).
[18] Minaxi Vinodkumar, K. N. Joshipura, C. G. Limbachiya, and B. K. Antony, Eur. Phys. J. D **37**, 67 (2006).
[19] K. N. Joshipura, Minaxi Vinodkumar, C. G. Limbachiya, and B. K. Antony, Phys. Rev. A **69**, 022705 (2004).
[20] K. N. Joshipura, M. Vinodkumar, B. K. Antony, and N. J. Mason, Eur. Phys. J. D **23**, 1 (2003).
[21] M. Vinodkumar, K. N. Joshipura, C. G. Limbachiya, and B. K. Antony, Nucl. Instrum. Methods Phys. Res. B **212**, 63 (2003).
[22] K. N. Joshipura, B. K. Antony, and V. Minaxi, J. Phys. B **35**, 4211 (2002).
[23] K. N. Joshipura, M. Vinodkumar, and U. M. Patel, J. Phys. B **34**, 509 (2001).
[24] K. N. Joshipura, Minaxi Vinodkumar, and P. M. Patel, Pramana, J. Phys. **43**, 495 (1994).
[25] D. R. Lide, *CRC Handbook of Physics and Chemistry*, 74th edition (Chemical Rubber Company, Boca Raton, FL, 1993–94).
[26] S. Hara, J. Phys. Soc. Jpn. **22**, 710 (1967).
[27] X. Zhang, J. Sun, and Y. Liu, J. Phys. B **25**, 1893 (1992).
[28] G. Staszewska, D. M. Schwenke, and D. G. J. Truhlar, Chem. Phys. **81**, 3078 (1984).
[29] G. P. Karwasz, R. S. Brusa, and A. Zecca, Riv. Nuovo Cimento **24**(1), 1 (2001).
[30] R. Basner, M. Schmidt, V. Tarnovsky, K. Becker, and H. Deustch, Int. J. Mass Spectrom. Ion Process. **171**, 83 (1997).
[31] C. Szymtkowski, Chem. Phys. Lett. **136**, 363 (1987).
[32] G. Garcia (private communication).
[33] H. C. Straub, B. G. Lindsay, K. A. Smith, and R. F. Stebbings, J. Chem. Phys. **108**, 109 (1998).
[34] A. Katase, K. Ishibashi, Y. Matsumoto, T. Sakae, S. Maezono, E. Murakami, K. Watanabe, and H. Maki, J. Phys. B **19**, 2715 (1986).
[35] A. Jain, J. Phys. B **21**, 905 (1988).
[36] F. A. Gianturco, J. Phys. B **24**, 3837 (1991).
[37] W. Hwang, Y. K. Kim, and M. E. Rudd, J. Chem. Phys. **104**, 2956 (1996).
[38] G. Vikor and M. V. Kurepa, J. Serb. Chem. Soc. **61**, 437 (1996).
[39] A. M. C. Sobrinho, N. B. S. Lozano, and M. T. Lee, Phys. Rev. A **70**, 032717 (2004).